VIP Cluster Compounds

DOI: 10.1002/anie.200705373

Intercluster Compounds Consisting of Gold Clusters and Fullerides: $[Au_7(PPh_3)_7]C_{60}\cdot THF$ and $[Au_8(PPh_3)_8](C_{60})_2$**

*Martin Schulz-Dobrick and Martin Jansen**

Recently, we started investigating the possibilities of synthesizing intercluster compounds,[1–3] which are well-defined arrangements of large, inorganic molecular units. At first, gold clusters and polyoxometalates were chosen as building blocks, owing to their stabilities and their variety in terms of shape, size, and ionic charge. In order to extend the choice of building blocks and to potentially induce interesting physical properties, fullerenes seem to be particularly attractive candidates to be included into intercluster compounds because of their electron-accepting properties. Depending on charge and counterions, a large variety of monomeric,[4–7] dimeric,[8–12] or polymeric[13] structures is realized in fulleride compounds, which can even be superconducting[14] or ferromagnetic.[15] However, successful crystallization of fullerides with other large, inorganic clusters has not been demonstrated to date, and it is supposed to be a challenging task. Fullerides are rather sensitive compounds; furthermore, it is not clear whether it is possible to obtain well-defined and ordered intercluster compounds, as the fullerene molecules often tend towards severe rotational disorder. Intercluster compounds that incorporate fullerides would be interesting not only owing to the generation of new arrangements of the fullerides themselves but also because of the possibility of charge transfer or hopping processes between different kinds of clusters.

Herein, the first intercluster compounds composed of gold clusters and fullerides are presented. Slow interdiffusion of solutions of $[Au_8(PPh_3)_8](NO_3)_2$ in acetonitrile and KC_{60} in THF leads to the separation of black crystals that contain gold clusters and fullerides. To date we have characterized two different compounds, $[Au_7(PPh_3)_7]C_{60}\cdot THF$ (**1**) and $[Au_8(PPh_3)_8](C_{60})_2$ (**2**).

The crystal structure of **1** was solved by single crystal X-ray diffraction[16] and consists of C_{60} monoanions and $[Au_7(PPh_3)_7]^+$ clusters. This cluster is depicted in Figure 1a and forms by a rearrangement reaction from the $[Au_8(PPh_3)_8]^{2+}$ cluster. One THF solvent molecule per formula unit is also incorporated in the lattice. The Au_7^+ cluster was structurally characterized previously,[17] and the central and peripheral Au–Au bond lengths in both compounds are in good agreement. The average bond lengths of the 6:6 bonds and the 6:5 bonds in C_{60}^- are 1.392(7) and 1.450(9) Å, respectively. The packing of the building blocks in the solid state is remarkable, owing to the segregation of the cations' and anions' partial structures. As can be seen from Figure 2, the gold clusters form double layers in such a way that they can be described as a section of the body-centered cubic packing with half of the unit cell. The fulleride ions form zigzag chains along [100] between the Au_7^+ double layers with center-to-center distances of 10.0 Å. In this structure, the fulleride ions do not dimerize, even at 100 K. The THF molecules are located within each layer of gold clusters, precisely in between two neighboring gold clusters along the [010] axis. A search for voids (PLATON[18]) reveals that the structure is closely packed and that no additional voids exist that could be potentially filled with solvent molecules.

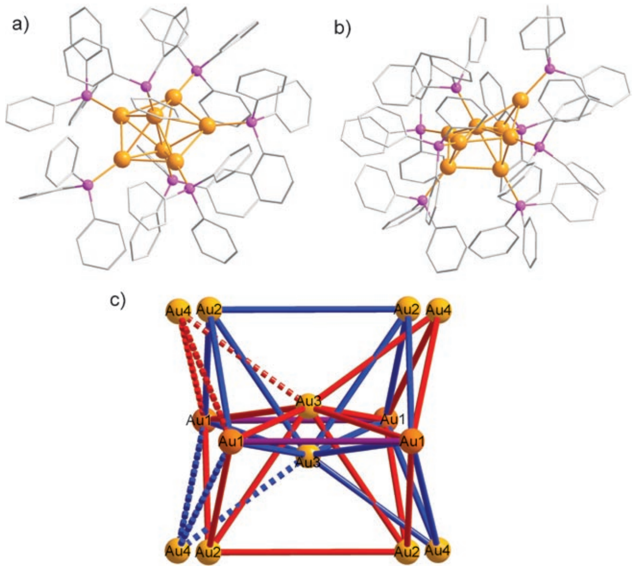

Figure 1. a) Structure of the $[Au_7(PPh_3)_7]^+$ cluster. b) Structure of the $[Au_8(PPh_3)_8]^{2+}$ cluster. Au yellow, P purple, C gray. c) Representation of the four orientations of the disordered Au_8 cluster in **2**. The red and blue orientations are related by a mirror plane through the Au1 atoms and the solid and dotted orientations by a mirror plane through the Au3 atoms.

The peculiar arrangement of the building blocks would certainly not be expected by just considering the Coulomb interaction and packing requirements such as size and shape of the building blocks, which would favor a CsCl- or NaCl-type packing. For intercluster compounds it has been demonstrated that local intermolecular interactions can play the decisive structure-directing role, even for more highly charged building blocks.[1] Thus, in the case of the large, singly-charged ions in **1**, this effect should be very likely to

---

[*] M. Schulz-Dobrick, Prof. Dr. Dr. h.c. M. Jansen
Max-Planck-Institut für Festkörperforschung
Heisenbergstrasse 1, 70569 Stuttgart (Germany)
Fax: (+49) 711-689-1502
E-mail: M.Jansen@fkf.mpg.de

[**] We would like to thank Alexandra Müller for preparative assistance, Dr. Reinhard K. Kremer for EPR measurements, and the Fonds der Chemischen Industrie for a scholarship.

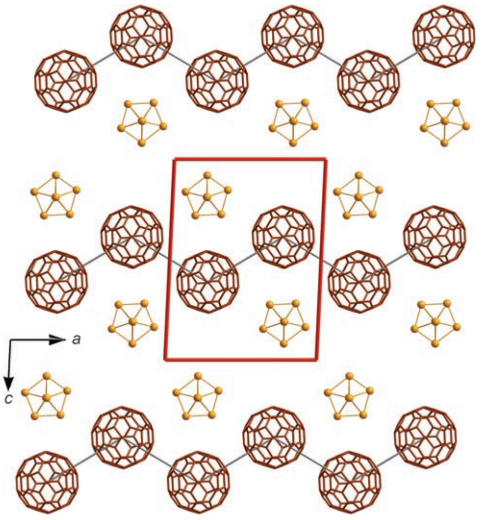

Figure 2. Projection of the crystal structure of **1** along [010]. The PPh_3 ligands are omitted for clarity. The unit cell is highlighted.

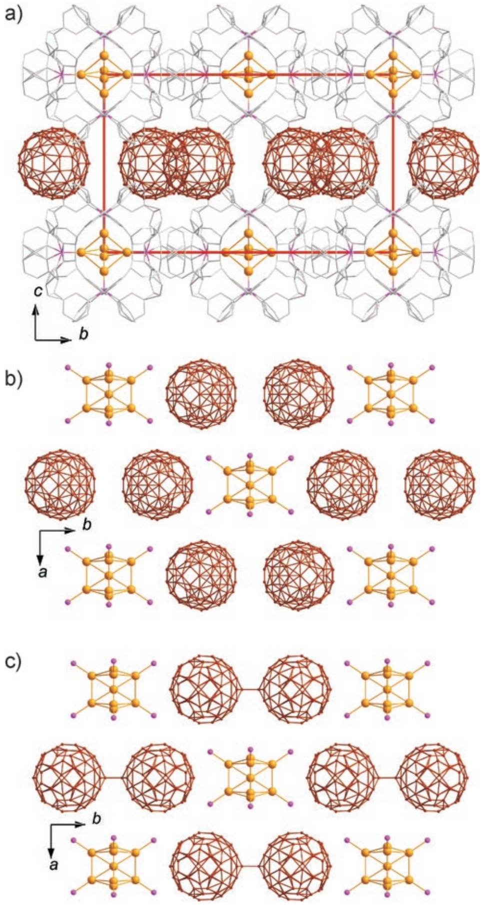

Figure 3. Projection of the crystal structure of **2** at 230 K a) along [100] and b) along [001]. c) Projection of **2** at 100 K along [001]. The phenyl rings are omitted in (b) and (c) for clarity.

occur as well. Indeed, a tendency towards close contacts within the cations' and the anions' partial structures (Au_7^+ double layers and C_{60}^- zigzag chains) is observed. This unfavorable electrostatic situation is energetically compensated by short-range attractive interactions, which are, in the case of the gold clusters, C–H–π contacts between the phenyl rings in the ligand periphery, while the fulleride unit are attracted by π–π interactions. The sum of these local interactions dominates the crystal structure, which fits well into our observations on other intercluster compounds.[1]

The crystal structure of **2** was solved and refined[16] in the orthorhombic space group *Cmmm*, in which the building blocks can only be described by a disordered model. Attempts to refine the structure without disorder in a space group of lower symmetry were not successful. The $[Au_8(PPh_3)_8]^{2+}$ cluster is depicted in Figure 1a. It is disordered over four orientations, with some atoms of different orientations sharing the same crystallographic sites. The superposition of the four different orientations leads to *mmm* symmetry (Figure 1c). The gold clusters form hexagonal layers with a primitive stacking in the crystal structure. The fullerene monoanions fill all trigonal-prismatic voids in this packing, leading to a layered structure in which cations and anions are packed as in the AlB_2-type structure (Figure 3). As discussed above for **1**, the separation of cations and anions into layers is evident and can be explained with the local interactions between the clusters of each layer. The crystal was measured at different temperatures. At 230 K the fulleride ions were found to be severely disordered. Their center-to-center distances within the layers are 9.80 Å along the [010] axis and 10.17 Å along the other directions. At 100 K, the fulleride cages were found to have dimerized through a covalent bond across the short intermolecular contacts (Figure 3c). The dimers are disordered over two orientations, which are related by a 180° rotation around the axis of the dimerizing bond. The structural transition is not accompanied by a change of space-group symmetry. Dimerization of fulleride monoanions is a well-known process that can occur at low temperatures in the solid state if the fullerides are in close enough contact.[8,12,19] Intercluster compounds often tend to incorporate substantial numbers of solvent molecules into the crystal structure, which could lead to a large decrease in crystallinity upon removal of the crystals from the mother liquor. A search for solvent-accessible voids in the crystal structure revealed only one small void per formula unit of suitable size to accommodate at most a single acetonitrile molecule. Thus, the crystals are stable outside the mother liquor.

The formation of different phases of gold clusters and fullerides is dependent on the reactant concentrations and the ratio of the two different solvents in the interdiffusion experiment. While the conditions could be optimized to reproducibly obtain **2** as a bulk material, as confirmed by powder X-ray diffraction, it was difficult to achieve full reproducibility for the crystallization of **1**. Therefore, only **2** was subject to further characterization.

Figure 4 displays the powder X-ray diffractogram of **2**, which is consistent with that calculated from the structural model and shows that the compound can be produced as a single phase that is stable upon removal of the mother liquor. The IR spectrum (Figure 4, inset) consists of a superposition of the bands of the gold clusters and the fullerides. The

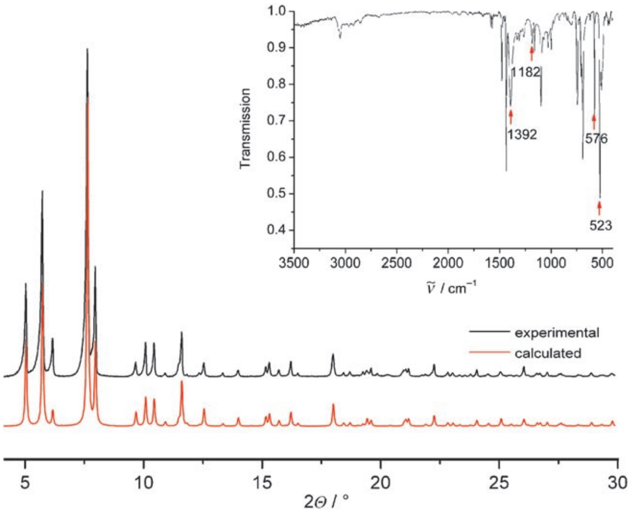

Figure 4. Comparison of the experimental and calculated powder X-ray diffractogram of **2**. The inset displays the IR spectrum of **2**. The red arrows mark the bands of the fulleride monoanions.

characteristic band at 1392 cm^{-1} confirms the presence of C_{60} monoanions.[20]

A powder sample of **2** was investigated by temperature-dependant EPR spectroscopy (Figure 5). At room temperature, the spectrum consists of two lines. The broad line ($\Delta H_{pp} = 51$ G) can be attributed to the C_{60} monoanions and the narrow line ($\Delta H_{pp} = 5.4$ G) to the inevitable impurity $C_{120}O$, which was investigated in detail previously.[21,22] With decreasing temperature, the ratio of the broad line to the narrow line gradually decreases, which can be attributed to the formation of diamagnetic fulleride dimers. However, no sharp transition temperature can be observed. In the spectrum at 10 K ($\Delta H_{pp} = 8$ G) the fulleride line, which decreases in width at low temperatures,[23] and the $C_{120}O$ line can no longer be distinguished. However, it is evident that a considerable proportion of C_{60} monoanions is present even at low temperatures. Either not all of the C_{60}^{-} ions in **2** form dimers, or an amorphous impurity phase is present, which contains structurally isolated C_{60} monoanions and cannot be detected in the powder X-ray diffractogram.

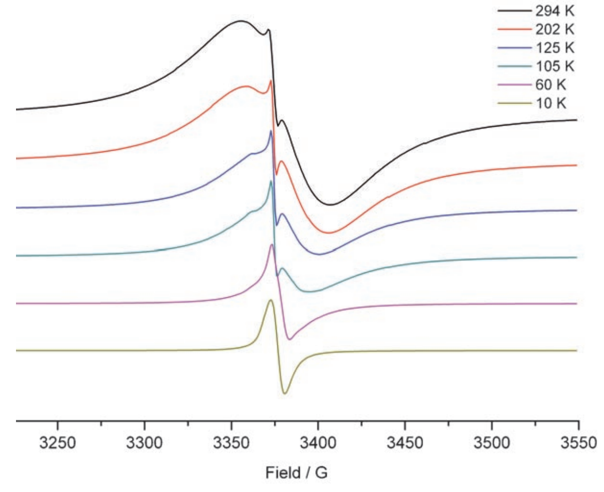

Figure 5. Temperature-dependant EPR spectra of **2**.

In summary, we demonstrate that it is possible to form intercluster compounds from gold clusters and fullerides. While some orientational disorder was observed in **2**, which is likely to occur owing to the spherical shape of the building blocks, the clusters are fully ordered in **1**. The employment of charged building blocks is clearly one of the significant driving forces for the formation of such intercluster compounds, and the long-range Coulomb interaction can be expected not only to contribute substantially to the total lattice energy but also to favor the formation of well-crystalline compounds. However, for the arrangement of the building blocks in the crystal structure, the short-range intermolecular interactions play the decisive role. The fulleride ions are arranged in zigzag chains in **1** and in layers in **2**, and such low-dimensional arrangements should therefore be favored employing large clusters as counterions. Thus, intercluster compounds offer good opportunities to obtain low-dimensional structures consisting of even more highly charged fullerenes, which could possess highly interesting electron-transport properties.

Experimental Section

THF and acetonitrile were dried with CaH_2 and distilled prior to use. A clear, dark purple solution of KC_{60} in THF (3 μmol mL^{-1}) was prepared by sonication of stoichiometric amounts of potassium and C_{60} in THF. $[Au_8(PPh_3)_8](NO_3)_2$ was prepared according to the literature.[24] All crystallization experiments were set up under argon in a drybox. The optimized conditions for the crystallization of **2** in bulk quantities, as checked by powder XRD, are as follows. In glass tubes of 15-mm diameter, $[Au_8(PPh_3)_8](NO_3)_2$ (36 mg, 9 μmol) in acetonitrile (6 mL) was underlayered with acetonitrile/THF (1:4, 5 mL) and KC_{60} in THF (3 μmol mL^{-1}, 5 mL). After one week, black crystals of **2** formed at the interface, and the solvent was removed. A single crystal was picked with a droplet of inert oil, transferred rapidly to the diffractometer, and measured at 100 K and 230 K. The material was ground for IR (KBr disks) and EPR spectroscopy (X-band) and powder XRD ($Cu_{K\alpha}$) measurements. The room-temperature cell parameters of **2** were determined by the Le Bail method to be $a = 1825.8(1)$, $b = 2864.3(1)$, and $c = 1752.3(1)$ pm. To find the optimal crystallization conditions of **2**, the concentrations of the components were varied. Occasionally, large, black, plate-shaped crystals of **1** appeared. However, we were not able to find the conditions for which the Au_8 cluster reproducibly rearranged into the Au_7 cluster to form compound **1**. For single crystal X-ray measurements, the crystals were transferred from the solvent into inert oil, picked with a loop, and cooled with liquid nitrogen to prevent the loss of included solvent molecules.

Received: November 22, 2007
Revised: December 17, 2007

Keywords: cluster compounds · EPR spectroscopy · fullerenes · gold · supramolecular chemistry

---

[1] M. Schulz-Dobrick, M. Jansen, *Inorg. Chem.* **2007**, *46*, 4380–4382.
[2] M. Schulz-Dobrick, M. Jansen, *Eur. J. Inorg. Chem.* **2006**, 4498–4502.

[3] M. Schulz-Dobrick, M. Jansen, *Z. Anorg. Allg. Chem.* **2007**, *633*, 2326 – 2331.

[4] A. Penicaud, A. Perezbenitez, R. Gleason, E. Munoz, R. Escudero, *J. Am. Chem. Soc.* **1993**, *115*, 10392 – 10393.

[5] P. Paul, Z. W. Xie, R. Bau, P. D. W. Boyd, C. A. Reed, *J. Am. Chem. Soc.* **1994**, *116*, 4145 – 4146.

[6] T. F. Fässler, R. Hoffmann, S. Hoffmann, M. Wörle, *Angew. Chem.* **2000**, *112*, 2170 – 2174, *Angew. Chem. Int. Ed.* **2000**, *39*, 2091 – 2094.

[7] T. F. Fässler, A. Spiekermann, M. E. Spahr, R. Nesper, *Angew. Chem.* **1997**, *109*, 502 – 504, *Angew. Chem. Int. Ed.* **1997**, *36*, 486 – 488.

[8] A. Hönnerscheid, L. van Wullen, M. Jansen, J. Rahmer, M. Mehring, *J. Chem. Phys.* **2001**, *115*, 7161 – 7165.

[9] D. V. Konarev, S. S. Khasanov, G. Saito, A. Otsuka, Y. Yoshida, R. N. Lyubovskaya, *J. Am. Chem. Soc.* **2003**, *125*, 10074 – 10083.

[10] D. V. Konarev, S. S. Khasanov, A. Y. Kovalevsky, G. Saito, A. Otsuka, R. N. Lyubovskaya, *Dalton Trans.* **2006**, 3716 – 3720.

[11] D. V. Konarev, S. S. Khasanov, A. Otsuka, G. Saito, R. N. Lyubovskaya, *J. Am. Chem. Soc.* **2006**, *128*, 9292 – 9293.

[12] D. V. Konarev, S. S. Khasanov, A. Otsuka, G. Saito, *J. Am. Chem. Soc.* **2002**, *124*, 8520 – 8521.

[13] P. W. Stephens, G. Bortel, G. Faigel, M. Tegze, A. Janossy, S. Pekker, G. Oszlanyi, L. Forro, *Nature* **1994**, *370*, 636 – 639.

[14] A. F. Hebard, M. J. Rosseinsky, R. C. Haddon, D. W. Murphy, S. H. Glarum, T. T. M. Palstra, A. P. Ramirez, A. R. Kortan, *Nature* **1991**, *350*, 600 – 601.

[15] P. W. Stephens, D. Cox, J. W. Lauher, L. Mihaly, J. B. Wiley, P. M. Allemand, A. Hirsch, K. Holczer, Q. Li, J. D. Thompson, F. Wudl, *Nature* **1992**, *355*, 331 – 332.

[16] Crystal data and structure refinement for **1**: black plate ($0.25 \times 0.15 \times 0.05\ \text{mm}^3$), triclinic, space group $P\bar{1}$, $a = 1720.1(1)$, $b = 1756.2(1)$, $c = 2434.3(2)$ pm, $\alpha = 110.071(1)$, $\beta = 91.569(1)$, $\gamma = 92.670(1)°$, $V = 6893(1) \times 10^6\ \text{pm}^3$, $\rho_{\text{calcd}} = 1.931\ \text{g cm}^{-3}$, $Z = 2$, $\mu(\text{Mo}_{\text{K}\alpha}) = 7.56\ \text{mm}^{-1}$, $\lambda = 71.073$ pm, Bruker AXS Smart APEX diffractometer, graphite monochromator, ω scan, semiempirical absorption correction (SADABS; G. M. Sheldrick, 2.10 ed., Bruker AXS, Madison, WI, USA, **2003**); structure solution and refinement with SHELXTL (G. M. Sheldrick, Version 6.10 ed., Bruker AXS, Madison, WI, USA, **2000**), $T = 100$ K, 59471 measured reflections, 30380 symmetry-independent reflections ($2\theta_{\text{max}} = 55.00°$), 1822 refined parameters, $R_1 = 0.0381$, $wR_2 = 0.0946$ ($F^2 > 2\sigma(F^2)$), $R_1 = 0.0437$, $wR_2 = 0.0978$ (all data). All non-hydrogen atoms were refined with anisotropic displacement parameters. The solvent molecule appears to be diffuse and was refined with isotropic displacement parameters and bond-length constraints. Crystal data and structure refinement for **2**: black rhombic crystal ($0.15 \times 0.12 \times 0.10\ \text{mm}^3$), orthorhombic, space group *Cmmm*, $Z = 2$, $\mu(\text{Mo}_{\text{K}\alpha}) = 6.51\ \text{mm}^{-1}$, $\lambda = 71.073$ pm, Bruker AXS Smart APEX diffractometer, graphite monochromator, ω scan, semiempirical absorption correction (SADABS); structure solution and refinement with SHELXTL, at $T = 230$ K: $a = 1832(1)$, $b = 2845(2)$, $c = 1756(1)$ pm, $V = 9150(12) \times 10^6\ \text{pm}^3$, $\rho_{\text{calcd}} = 1.761\ \text{g cm}^{-3}$, 40504 measured reflections, 5998 symmetry-independent reflections ($2\theta_{\text{max}} = 56.70°$), 144 refined parameters, $R_1 = 0.0879$, $wR_2 = 0.2378$ ($F^2 > 2\sigma(F^2)$), $R_1 = 0.1108$, $wR_2 = 0.2648$ (all data). The gold cluster is disordered over four orientations. The phenyl rings were refined with anisotropic parameters and restrained to regular hexagons. The disorder of the fullerene molecule could not be fully resolved. All carbon atoms were refined with half occupancy and isotropic displacement parameters. Crystal data and structure refinement for **2** at 100 K: $a = 1828.1(1)$, $b = 2816.5(2)$, $c = 1750.6(1)$ pm, $V = 9013(1) \times 10^6\ \text{pm}^3$, $\rho_{\text{calcd}} = 1.788\ \text{g cm}^{-3}$, 39806 measured reflections, 5877 symmetry-independent reflections ($2\theta_{\text{max}} = 56.66°$), 140 refined parameters, $R_1 = 0.1005$, $wR_2 = 0.2617$ ($F^2 > 2\sigma(F^2)$), $R_1 = 0.1185$, $wR_2 = 0.2824$ (all data). The gold cluster is disordered over four orientations. The phenyl rings were refined with anisotropic parameters and restrained to regular hexagons. The fulleride dimers are disordered over two orientations and were refined with isotropic displacement parameters. CCDC 668368 (**1**), 668369 (**2** at 100 K), and 668370 (**2** at 230 K) contain the supplementary crystallographic data for this paper. These data can be obtained free of charge from The Cambridge Crystallographic Data Centre via www.ccdc.cam.ac.uk/data_request/cif.

[17] J. W. A. van der Velden, P. T. Beurskens, J. J. Bour, W. P. Bosman, J. H. Noordik, M. Kolenbrander, J. Buskes, *Inorg. Chem.* **1984**, *23*, 146 – 151.

[18] A. L. Spek, Utrecht University, **2005**.

[19] G. Oszlányi, G. Bortel, G. Faigel, L. Granasy, G. M. Bendele, P. W. Stephens, L. Forro, *Phys. Rev. B* **1996**, *54*, 11849 – 11852.

[20] C. A. Reed, R. D. Bolskar, *Chem. Rev.* **2000**, *100*, 1075 – 1119.

[21] P. Paul, K. C. Kim, D. Y. Sun, P. D. W. Boyd, C. A. Reed, *J. Am. Chem. Soc.* **2002**, *124*, 4394 – 4401.

[22] P. Paul, R. D. Bolskar, A. M. Clark, C. A. Reed, *Chem. Commun.* **2000**, 1229 – 1230.

[23] P. M. Allemand, G. Srdanov, A. Koch, K. Khemani, F. Wudl, Y. Rubin, F. Diederich, M. M. Alvarez, S. J. Anz, R. L. Whetten, *J. Am. Chem. Soc.* **1991**, *113*, 2780 – 2781.

[24] J. W. A. van der Velden, J. J. Bour, W. P. Bosman, J. H. Noordik, *Inorg. Chem.* **1983**, *22*, 1913 – 1918.